Int. J. Environ. Sci. Technol. (2016) 13:803–812
DOI 10.1007/s13762-015-0910-2

ORIGINAL PAPER

Optimization of sulfur adsorption over Ag-zeolite nanoadsorbent by experimental design method

G. Bakhtiari[1] · M. Abdouss[1] · M. Bazmi[2] · S. J. Royaee[2]

Received: 18 January 2015 / Revised: 23 August 2015 / Accepted: 18 November 2015 / Published online: 11 January 2016

Abstract Environmental protection has mentioned the need to cut out all of fuels sulfur compounds. One of the most important processes that affect sulfur removal in atmospheric condition is the interaction of liquid fuels with solid sulfur removal adsorbents such as zeolites. To investigate the nano-AgX-zeolite efficiency for the sulfur adsorption process, a set of experimental tests was arranged and conducted by Box–Behnken design software, in an adsorption laboratory setup. The selected variables comprised metal percent, adsorption temperature and calcination temperature. The parameter levels were 0.5–10 %, 30–120 and 200–500 °C, respectively. The experiment results were used to find the statistical model. The results demonstrate that the sulfur concentration level is 48.36 ppm in the last product at 83 °C for adsorption temperature, 5.53 % for metal percent and 436 °C for calcination temperature in constant pH and constant process time.

Keywords Adsorption · Desulfurization · Experimental design · Zeolite · Synthesis

✉ M. Abdouss
phdabdouss44@aut.ac.ir

[1] Chemistry Departments, Amirkabir University of Technology, P.O. Box 15875-4413, Tehran, Iran

[2] Refining Technology Development Division, Research Institute of Petroleum Industry, Tehran, Iran

Introduction

In recent years, more strict rules have been developed to reduce transportation fuels sulfur levels for environmental protection purposes. Hydro desulfurization (HDS) is an effective method for removing mercaptans and sulfides, but this method is not suitable for the thiophenic compounds removal. For instance, H_2S generated in some thiophene compounds reaction is a major inhibitor for ultra-deep hydrodesulfurization (UDHDS) of non-reactive varieties (Gutiérrez et al. 2014; Zepeda et al. 2014). Recent studies have shown that σ-complexation in adsorbent is a greater adsorption force than other forces for this main application. Molecular orbital calculation has noticed that the σ-complexation bond between metals such as Ag+ and thiophene is the greatest force with aromatics, for example benzene. Therefore, σ-complexation adsorbent is delicate in fuels sulfur removal (Yi et al. 2013; Yang et al. 2002; Salmasi et al. 2013; Hernández-Maldonado and Yang 2003). The detailed discussion for liquid fuel desulfurization by adsorption is reviewed from many sources (Yang 2003). Ma et al. (2002, 2005) investigated thiophenic compounds adsorption by fixed-bed reactor from gas oil and jet fuels, using silica gel with 5 wt% loading of transition metal compound. This study was also done only for 4,6-dimethyldibenzothiophene and dibenzothiophene (DBT) molecules removal. MIP, polymer nanofiber and fruit wastes are used to create specific molecular recognition sites to identify molecules of sulfur compounds template (Yong et al. 2014; Ogunlaja et al. 2014; Ahmed and Ahmaruzzaman 2015). Collins et al. (1997) used adsorption experiments by fixed-bed reactor for sulfur compounds removal after thiophenic compounds oxidation. Oxidation reaction requires agents such as

H_2O_2, catalyst (acid) and a transfer between two phases (inorganic and organic). Other adsorbents such as activated alumina have been investigated by Alcoa Selexsorb research team. This activated alumina has applications in some processes (Irvine 1998) and ability of hetereoatoms adsorption and naphtha production with 30 ppm sulfur.

One of the famous materials used in some compounds removal from liquid and gas phases is zeolite. Organic solvents and transportation fuels were treated by zeolites in attaining high quality and price. Hence, a lot of efforts were made to find a proper precursor and modify present techniques to gain zeolites with specific applications (Houthoofd et al. 2008; Moattar and Hayeripour 2004). Today, zeolite productions have been developed due to having a great amount of resources, low costs and increasing applications in industries (Wajima and Ikegami 2009; Tian et al. 2014).

According to the scientists' viewpoint, it is important to explain about the zeolite with improved structure and high adsorption of thiophenic compounds. Thiophene has sulfur atom electrons and its two lone pairs: one of them lies on π system electron, and the other lies on the ring plate. This molecule has two *n*-type donating electrons, and lone pair electrons lie in the ring plate of to adsorbent (sigma bond of metal–sulfur). Also π-type donating electrons by π electrons of the ring (π bond in metal complex) occur in thiophene molecule. Thiophene adsorption on improved zeolite (AgX-zeolite) occurs on the basis of hard/soft acids and bases rules. These explain that hard acids are related to hard bases and soft acids are related to soft bases. Hence, a silver ion is a soft acid that has high performance in valence electrons polarization and is related to soft bases (such as thiophene). On the other hand, silver ion can create π complex with thiophene by π-type bonds. Ag-zeolite has high adsorption of thiophene because of thiophene as a soft base related to Ag as a soft acid (Ma et al. 2005; Hernandez-Maldonado and Yang 2004; Yang and Hernandez-Maldonado 2003; Hernández-Maldonado and Yang 2003; Gong et al. 2009; Laborde-Boutet et al. 2006; Qin et al. 2014).

The present paper aim is based on the investigation of parameters with mutual effects, to improve sulfur compounds adsorption and finding the best adsorption condition. The specific aim of this study is to optimize the experimental conditions that maximize the adsorptive capacity of synthesized X-zeolite. This is done in nanoscale (by nanosilver ions) for desulfurization process design and by the use of the BBD design method (Bagheri et al. 2012; Kumar et al. 2008; Dutta 2013; Kumar and Srivastava 2012; Sumathi et al. 2009; Mourabet et al. 2012). This study was carried out in winter 2015 in Amirkabir University.

Materials and methods

Material

Chemical compounds that used in experimental step were pure, completely and directly used in reactions. NaOH tablets (99 %), anhydrous $NaAlO_2$, SiO_2 as an aqueous solution (30 wt%) were attained from Aldrich.

*Iso*octane (99 wt%), thiophene (98 wt%) and $AgNO_3$ (99.9 wt%) were purchased from Merck.

Physical and chemical analysis

Bruker D8 Advance with Cu KR monochromatic source, scanning 0.05°/0.2 s that worked at 30 mA, 40 kV used for XRD (X-ray diffraction) plans and Optima 2000DV from Perkin-Elmer factory specified zeolite Chemical compositions.

N_2 isotherms were determined by the Micromeritics device (ASAP 2020) at 77 °K. The first samples were degassed at 305 °C for 12 h in 0.01 Pa constant vacuums. The information attained from isotherms was used for determination of DFT (pore size distribution), S (specific surface area), V_t (total pore volume), L_{mic} (average micropore size) and V_{mic} (micropore volume).

A gas chromatography device used for determination of thiophene concentration in adsorption experiments was Shimadzu GC-17A with FPD detector (flame photometric detector), 30-m capillary column EC-5, 32×10^{-2} mm diameter. The oven temperature was raised to 190 °C from 50 °C (5 °C/min), and the injector temperature was 70 °C. The retention time for thiophene was 7 min (thiophene dissolved in isooctane).

The last results that used in this study are like others. The limitation of thiophene concentration in solution is determined after injection of different concentration solutions in GC; 0.56 ppm sulfur was the least detection level for detector in this device. Below this level, noise was appeared.

Vertex-70 from Bruker factory was used for FT-IR (Fourier transform infrared spectroscopy) tests that had a small cell and combine reactor.

Transmission electron microscopy (TEM) was carried out in a Zeiss EM10C-100 kV microscope.

Experimental

Synthesis and improvement of nanoadsorbents

Anhydrous $NaAlO_2$ as an alumina source and SiO_2 (colloidal, 30 wt%) as a silica source were selected. Produced hydrogel with 3.4 Na_2O:2.9 SiO_2:Al_2O_3:150 H_2O molar ratio was applied for the X-zeolite synthesis in proportional temperature. In the first step, $NaAlO_2$ was added to NaOH solution prepared from NaOH tablets in water, and then colloidal SiO_2 was added to the first step solution for attaining hydrogel. After mixing hydrogel for 45 min at an ambient temperature, hydrogel transfers to Teflon hydrothermal reactor for 22 h in 108 °C in immobility condition. Then synthesized solids were filtered and washed with water (deionize) until pH reaches about 8. Finally, the products were dried in air atmosphere for 26 h at 100 °C (Kostinko 1982).

Initially, adsorbents were prepared by impregnation of zeolite with an aqueous solution of $AgNO_3$ (99.9 %) aiming at introducing 5.53 % of metal of adsorbent (sample named AgX-zeolite). The impregnation was performed in a rotary evaporator at 50 °C for 2 h. Finally, the material was calcined at 436 °C in a furnace under atmospheric air, for 4 h (2 °C/min rate) after drying at 100 °C. In this work, these samples are identified as modified nanoadsorbents.

Adsorption study

All of the experimental tests that used for measuring the adsorption performance were in a batch reactor. Produced feed was mixed 432 ppm sulfur as thiophene in *iso*octane that used as a model feed of naphtha; 10 mL from model feed with 0.5 g from selected adsorbent is put in stainless steel reactor (50 mL) and shaken for 4 h (constant time) in desired temperatures. The process time was investigated in several times. Finally, the results were analyzed and the best time was selected (Fig. 1). After the test, adsorbents are filtered and liquid product injected to sulfur analyzer (GC) for the determination of sulfur concentration.

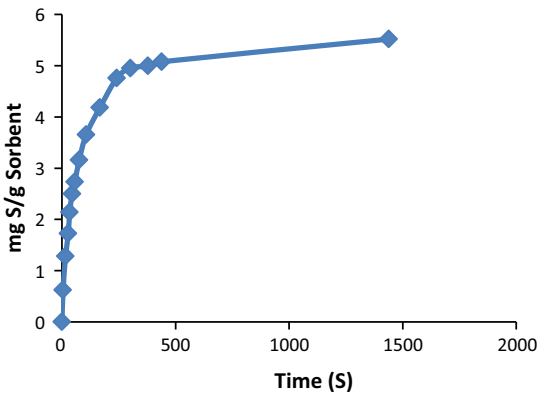

Fig. 1 Effect of contact time on uptake of sulfur compound feed

Experimental design

The statistical methodology was used for the optimization of thiophene adsorption on X-zeolite. The Box–Behnken method was selected for the investigation of factors effect: adsorption temperatures (°C), calcinations temperatures (°C) and metal percent (%) as shown in Table 1. The two *K* factors need for three levels of rotatable factors. All of the factors were investigated at −1, 0, +1, levels. Center points inclusion suggested a more precise approximation of error in experimental answers and produced a measure for the suitability of the model (lack of fit). On the other hand, this model can determine the importance of factors interaction. Investigated factors level and similarity between coded and actual types are shown in Table 2.

Results and discussion

Nanoadsorbent characterization

The synthesized zeolite is white color, but after Ag impregnation and calcinations, its color changed dark. The synthesized zeolite XRD and improved adsorbent pattern that calcined at 436 °C are shown in Fig. 1. XRD patterns show several index peaks at 2.18°, 2.79°, 2.89°, 3.33°, 3.79°,7.55°, 8.94°, 14.16° and 38.10°, 44.30°, 64.50°, 78.30° Å (Cheng et al. 2015; Wajima and Ikegami 2009; Zhang et al. 2013). The same parameters in XRD patterns and Table 3 exhibited similarities between AgX-zeolite

Table 1 Experimental ranges and levels in the experimental design

Variable	Factors	Range and level		
T adsorption (°C)	*A*	30	75	120
Metal %	*B*	0.5	5.25	10
T calcination (°C)	*C*	200	350	500

Table 2 All of factorial design used for adsorptive desulfurization using AgX-zeolite

Std	Run	T adsorption (°C)	Metal %	T calcination (°C)	$Y_{exp.}$ (ppm)	$Y_{pre.}$ (ppm)
8	1	120	5.25	500	52	48.75
6	2	120	5.25	200	131	126.5
17	3	75	5.25	350	51	56.4
11	4	75	0.5	500	108	102.87
2	5	120	0.5	350	113	121.38
13	6	75	5.25	350	52	56.4
15	7	75	5.25	350	70	56.4
10	8	75	10	200	117	122.13
1	9	30	0.5	350	112	112.63
7	10	30	5.25	500	74	78.5
16	11	75	5.25	350	54	56.4
3	12	30	10	350	101	92.63
12	13	75	10	500	93	96.88
4	14	120	10	350	62	61.37
14	15	75	5.25	350	56	56.4
5	16	30	5.25	200	116	119.25
9	17	75	0.5	200	200	196.13

Table 3 Physical and chemical properties of calcined X-zeolites, metal-impregnated zeolite

Sample	Metal ion	Metal-impregnated (%)	Si/Al	M/Al	S_{BET} (m^2/g)	V_t (cm^3/g)	L (nm)
NaX-zeolite	Na	0	1.086	–	691.52	0.3577	2.0688
AgX-zeolite	Ag	5.53	1.031	0.297	230.16	0.1826	3.1729

L, average pore size (nm), V_t, total pore volume (cm^3/g), S_{BET}, BET area (m^2/g)

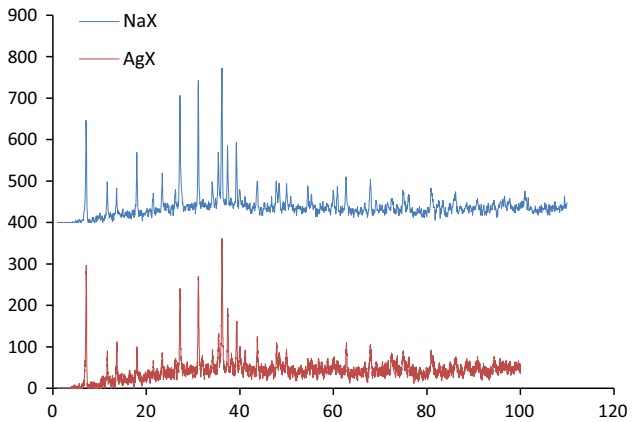

Fig. 2 XRD patterns of AgX-zeolite and original NaX-zeolite

and synthesized X-zeolite structure without any change in crystals after metal impregnation and heat process in a furnace. This information has shown that metal ions did not make zeolite structures unstable. Synthesized and impregnated zeolite compositions are shown in Table 3. Measurement of Si, Al elements and their ratio in metal-impregnated zeolite and original case are similar to each other. AgX-zeolite has a stable structure because of the metal-Al ratio is existed without any change in its structure. This point shows that Al disintegration in impregnation step occurs rarely. All analyses showed impregnation, and calcination processes were successful without any change in zeolite chemical structure.

The FT-IR spectra of the synthesized X-zeolite, AgX, are shown in Fig. 2. The FT-IR spectra of the synthesized X-zeolite and AgX corresponded to the zeolite X's characteristic peak. Zeolite X has the main characteristics of skeletal vibration peak: tetrahedron stretching vibration peak at 975 with a shoulder at 1053, 750, 668 cm^{-1}; double 6-ring vibration peak of 562 $cm^{-1}$and T–O bending vibration peak of 459 cm^{-1} and a peak at 3467 cm^{-1} indicated the Si–OH on the structure of zeolite, and zeolite AgX has the main characteristic of peak at 616 cm^{-1}. The IR analysis demonstrated that the impregnating Ag ion on synthesized X-zeolite has little effect on the zeolite chemical structure. The FT-IR spectra of the NaX, AgX-

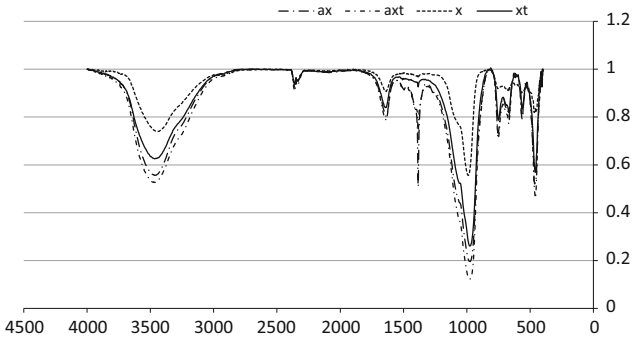

Fig. 3 FT-IR spectra of 13X zeolite (**a**), FT-IR spectra of adsorbed thiophene over 13X zeolite (**b**), FT-IR spectra of Ag-13X zeolite (**c**), and FT-IR spectra of adsorbed thiophene over Ag-13X zeolite (**d**)

zeolites, before adsorbing the thiophene (a, c) and after adsorption of the thiophene (b, d), show a contrast between (a, c) and (b, d). The band at 2924 and 2863 cm^{-1}can be observed in (b, d) which is assigned to the C−H stretching vibration of saturated CH_3 and CH_2, indicating some of the adsorbed thiophene can undergo the opening of its thiophenic ring in adsorption processes, the change on the molecular structure has taken place (Song et al. 2014; Shi et al. 2013; Balkus and Ly 1991).

The adsorption isotherm for sulfur compounds adsorption on AgX-zeolite is shown in Fig. 3. The isotherm presents a Langmuir model ($C_s/q = 1/(Q_m b) + C_s/Q_m$) behavior (Shams et al. 2008; Song et al. 2015) to study model feed. The results of adsorption experiments use 0.2 to 0.7 g of adsorbent and 10 mL model feed which are shown in Fig. 3b (adsorption constant), Q_m (saturation capacity) are calculated for the sulfur compounds adsorption, respectively, 3.648 mg/g and 0.133 mL/mg. Its correlation coefficient is 0.99, and this indicator by Freundlich model is 0.94. Therefore, the isotherm of AgX-zeolite was well described by the Langmuir model and fitted its curve by the Langmuir model for AgX-zeolite which shows that the Langmuir model described the thiophene molecule adsorption. The best performance was achieved by AgX-

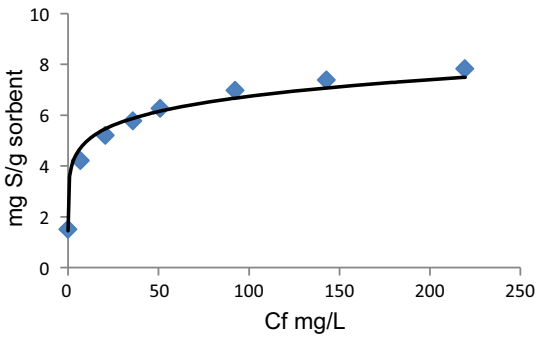

Fig. 4 Langmuir adsorption isotherms of adsorbent

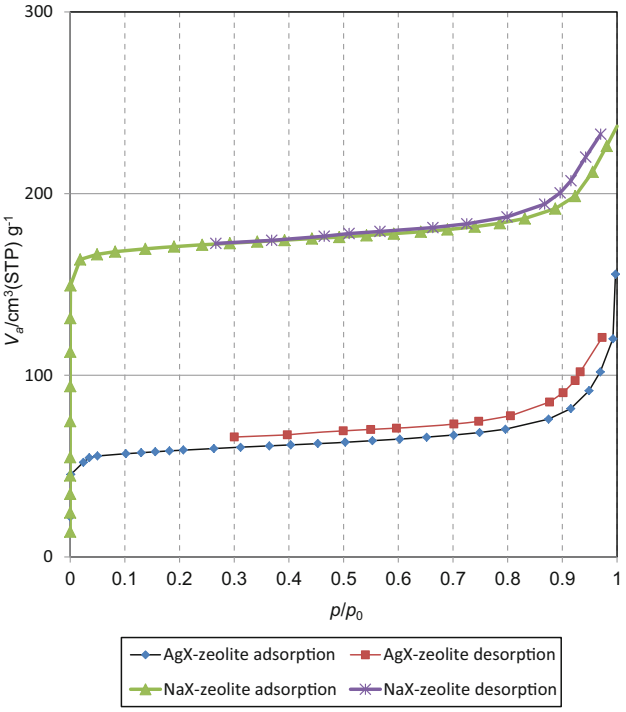

Fig. 5 Nitrogen adsorption/desorption isotherms. *Star* NaX-zeolite desorption, *triangle* NaX-zeolite adsorption, *big square* AgX-zeolite desorption, *small square* AgX-zeolite adsorption

zeolite, and for sulfur adsorption, enhancing the adsorption capacity of AgX-zeolite was high (about 8 mg s/g sorbent).

Pore structure characterization in the nanoadsorbents

Pore structures play the important role in the adsorption performance of adsorbents (AgX-zeolite) due to the complex formation on surface chemistry. The isotherms of N_2 adsorption/desorption in NaX-zeolite and AgX-zeolite at 77 °K are noticed in Fig. 4. Figure 5 shows the pore size distributions for NaX-zeolite and AgX-zeolite that pore size distribution and isotherms were used to attain this information. The super mesopores were noticed on the NaX-zeolite and AgX-zeolite clearly. BJH (Barrett–Joyner–Halenda) showed uniform mesopore distribution (size = 2 nm) and suitable analysis of isotherms desorption branch. Table 3 shows the NaX-zeolite and AgX-zeolite main characters. The Brunauer, Emmett and Teller (BET) was determined specific surface area of porous material such as zeolite adsorbents in special pressure range between 1×10^{-2} and 25×10^{-2}. Figure 4 shows total pore volume about 0.99 by estimating via using the (BET) equation in the relative pressure ranges (*P*/*P*0) from 0.01 to 0.25, and V_t Fig. 4 shows the total pore volume via adsorption isotherm by estimation process. Total pore volume of adsorbent is completely filled with liquid N_2 in

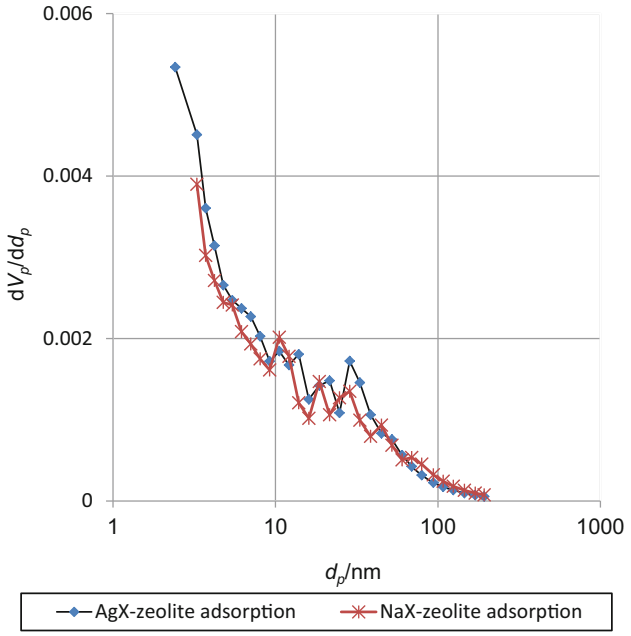

Fig. 6 pore size distributions for the adsorbents. *Star* NaX-zeolite adsorption, *square* AgX-zeolite adsorption

boiling operation condition. Eventually, pores volume and total area of NaX-zeolite were larger than those of AgX-zeolite. Hence, the NaX-zeolite pore size was smaller than AgX-zeolite. The best pore size is assisted with sulfur removal in the adsorption process (Fig. 5).

X-zeolite particular structure as a support and the Ag-adsorbent were studied by SEM in Fig. 6a, b, respectively. In calcined AgX-zeolite adsorbent that is shown in SEM images, impregnated silver ions on NaX-zeolite (calcination at 436 °C). Improved adsorbent demonstrates a cubic shape and regular crystal structure with sharp angles that were completely coated with silver (Fig. 6a).

Figure 7a shows zeolite surface with precipitation of nanocluster of silver that was impregnated on NaX-zeolite (Fig. 7b); average nanocrystal size was about ~5–8 nm (Fig. 7a).

Various parameters effect on thiophene removal efficiency

To predict the ideal conditions for thiophene adsorption on the adsorbents, the main points were given to software (Box–Behnken) that contributed to the central point; fit brief of product exhibits that the adsorbent in this system produced from high efficiency and benefit model. The ratio statistical implication of the mean square changes due to the mean square error, and regression was tested by the ANOVA (variance investigation). ANOVA is a statistical technique that subdivides the total variation in a set of data in parts associated with specific sources of variation for the purpose of testing hypotheses on the model parameters. Table 4 information indicates that the ANOVA analysis, which is the most important individual effect for AgX-zeolite adsorption of thiophene, was the metal percent ($P = 0.0003$) followed by the calcination temperature ($P < 0.0001$) and adsorption temperature ($P = 0.1092$). Investigation of factors mixed effect and experimental tests were performed for the mixing parameters by designed experiment tests statistically. Responses (Y) for thiophene adsorption on AgX-zeolite are listed in Table 2 according to its matrix.

The amount of the predicted thiophene removal and the real values are shown in Fig. 8, although these values are less than MIP adsorbents, but the present adsorbent can remove the complex of fuels sulfur compounds simultaneously (Yong et al. 2014) and this adsorbent has a better performance and higher efficiency about 60 % rather than other zeolite adsorbents. (Tian et al. 2014; Qin et al. 2014) In this plot, data points lie on acceptable near to a direct line. Experimental level of investigation distributes completely. The real thiophene removal measure is the

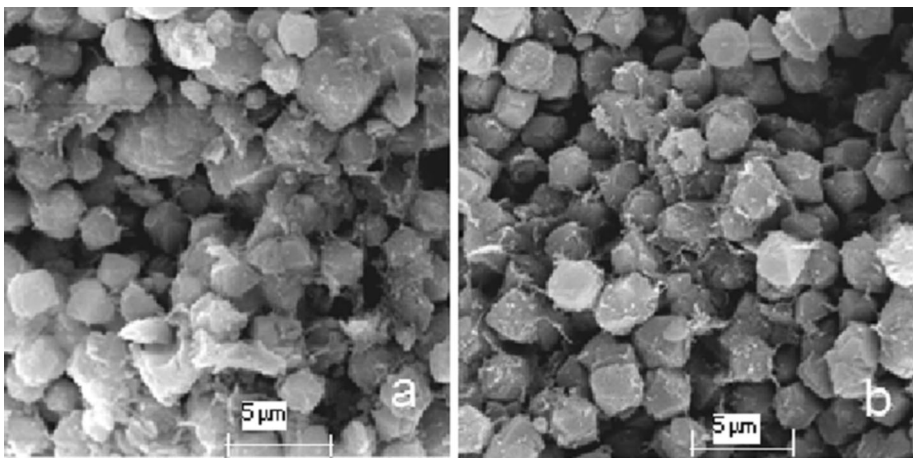

Fig. 7 **a** SEM image of calcined Ag-impregnated sorbent based on X-zeolite and **b** SEM image of X-zeolite

Table 4 ANOVA for response surface quadratic model (*Y*)

Source	Sum of squares	d.f.	Mean square	*F* value	*P* > *F*	Remark
Model	24,440.02	9	2715.56	36.11	<0.0001	Significant
A-temp	253.13	1	253.13	3.37	0.1092	
B-metal %	3200	1	3200	42.55	0.0003	
C-calcination	7021.13	1	7021.13	93.36	<0.0001	
AB	400	1	400	5.32	0.0545	
AC	342.25	1	342.25	4.55	0.0703	
BC	1156	1	1156	15.37	0.0057	
A2	19.92	1	19.92	0.26	0.6227	
B2	6216.76	1	6216.76	82.66	<0.0001	
C2	5062.55	1	5062.55	67.31	<0.0001	
Residual	526.45	7	75.21			–
Lack of fit	285.25	3	95.08	1.58		Not significant
Pure error	241.2	4	60.3			–
Cor. total	24,966.47	18				–

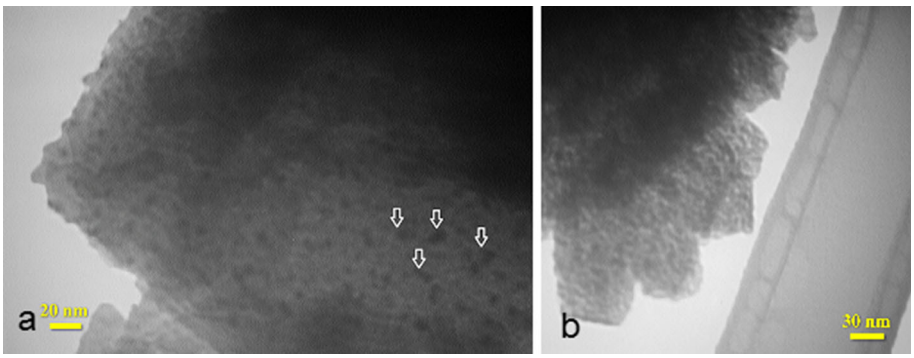

Fig. 8 TEM images of **a** AgX-zeolite and **b** parent NaX-zeolite

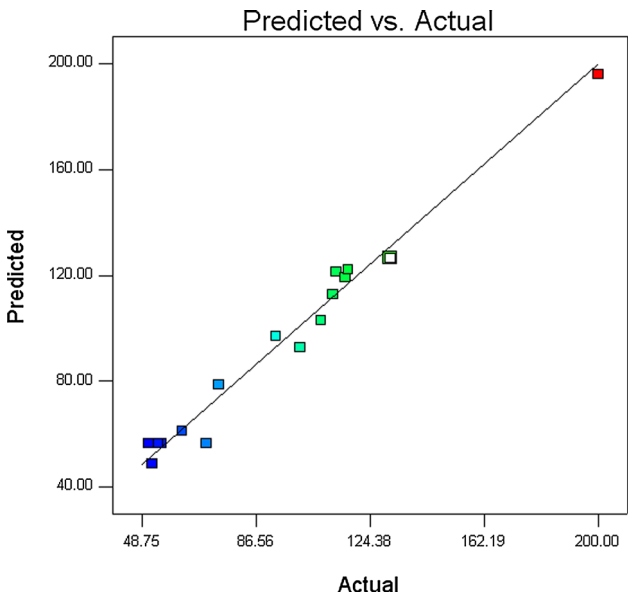

Fig. 9 Scatter diagram of predicted response versus real response for adsorption of thiophene on zeolite

determined result in the special run, and the foreseen measure is investigated by the autonomous variables in the BBD.

The results demonstrated that the thiophene adsorption capacity of AgX-zeolite raised by raising adsorption temperature. Again, it was observed that with the raising calcination temperature, the thiophene adsorption increases with the surface area of zeolite which has more adsorptive sites. The metal percent on zeolite plays a vital role irrespective of the other experimental parameters with increasing adsorptive sites and metal–sulfur interactions (Fig. 9). A rule for foreseeing connection among the factors, responses and interactions is by examining plots. In this analysis method, each contour demonstrates some mixture of two variables with others at several quantities. The response surface contours were plotted against measure of calcination temperature/metal percent, adsorption temperature/metal percent and calcination temperature/adsorption temperature as shown in Fig. 10. The interaction between metal percent and calcination

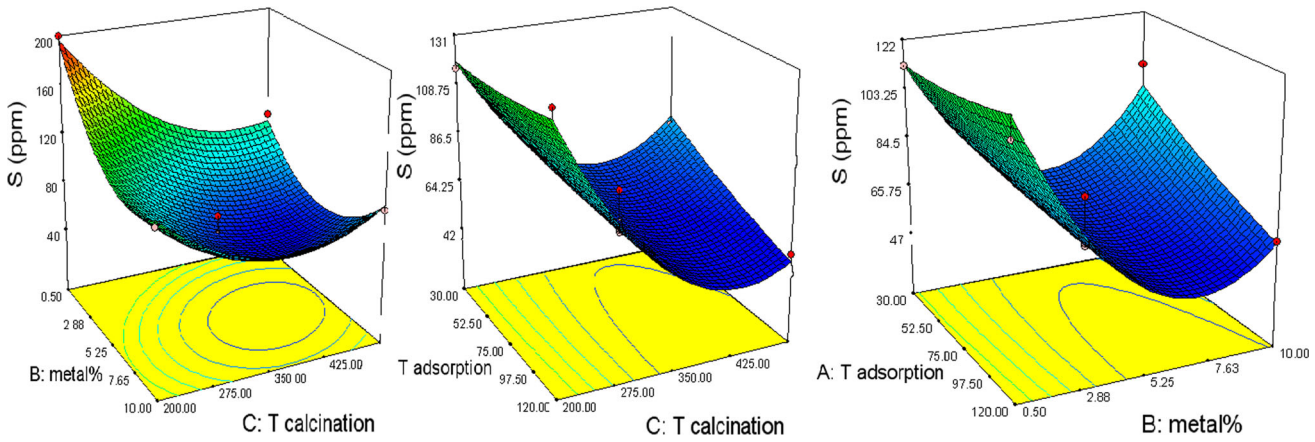

Fig. 10 Response surface graph in three dimensions for sulfur removal versus metal percent, calcination temperature and adsorption temperature for thiophene–zeolite adsorption system

temperature was vital dual effect ($P < 0.0057$). The interaction between metal percent and adsorption temperature was the second vital effect ($P = 0.0545$), and interaction between calcination temperature and adsorption temperature was the least effect ($P = 0.0703$). The highest measure of the adopted determination coefficient (R^2 Adj = 0.9789) was recorded. This result denoted of total variation on thiophene adsorption information that explained by chosen model is about 97.89 %. The suitable precision ratio that is about 22.157 shows suitable signal-to-noise ratio. Hence, coefficient adopted the determination in model is about 70 % and suitable precision ratio is more than 4. Produced model used in the design space and determined process provides excellent conditions. Calcination temperature and metal percent had the most significant effects on thiophene adsorption at calcination temperature of 436 °C with metal percent, 5.53 %, and the model predicted thiophene adsorption efficiency is close to 50 ppm on AgX-zeolite, because the level of calcination temperature, adsorption temperature and metal percent were optimized for high adsorption.

After searching between 17 starting points, the best answer was selected (Fig. 10). Produced information was in the tests that related to demonstrated BBD results by suitable functions could help for the adsorption parameters in thiophene removal.

This method with response surface appliance developed predictable parameters indicated an experimental relationship between the opinion variables expressed and the response by the following fitted second-order polynomial equation:

$$Y = 56.4 - 5.62A - 20B - 29.63C - 10AB - 9.25AC + 17BC + 2.18A^2 + 38.4B^2 + 34.68C^2$$

Experimental regeneration

A regeneration process for situation AgX-zeolite that situated by sulfur compounds was performed in hot air (210 °C) for 1 h. Regenerated AgX-zeolite performance was used five times as a fresh adsorbent and was given the best performance.

Conclusion

According to the BBD method design, 21 experimental tests were considered to determine the effects of metal percent, calcinations temperature, adsorption temperature and their desulfurization ability via an adsorption process. The method and experimental results were scrutinized by statistical analyses for determination of interaction parameters. According to results, two parameters that have the best interaction with the adsorption process are metal percent and calcination temperature. 3D diagrams in software and contours demonstrate method results summary on response surface. Also increasing the metal percent causes diminishing the adsorption ability. Therefore, this factor has a lower convergence tendency in responses. The

Table 5 Best operating condition for produced adsorbent

Name	Temperature (°C)	Calcination (°C)	Metal %	Sulfur (ppm)
AgX-zeolite	83	436	5.53	50

calcination temperature results in a better adsorption and causes a higher desulfurization. More metal percentage and adsorption temperature increase the adsorption ability.

According to the experimental design best condition, calcination temperature, adsorption temperature and metal percentage for the best adsorption are 436, 83 °C and 5.53 %, respectively, and this adsorbent had 3 % difference in predicted performance (Table 5). The simulation and experimental results can be applied in refineries desulfurization, process for sulfur removal development.

Acknowledgments The authors wish to thank Chemistry Departments, Amirkabir University of Technology, Tehran, Iran, and Refining Technology Development Division, Research Institute of Petroleum Industry, Tehran, Iran, for their assistance.

References

Ahmed MJK, Ahmaruzzaman M (2015) Adsorptive desulfurization of feed diesel using chemically impregnated coconut coir waste. IJEST 12(9):2847–2856

Bagheri A, Taghizadeh M, Behbahani M, Asgharinezhad A, Salarian M, Dehghani A, Ebrahimzadeh H, Amini M (2012) Synthesis and characterization of magnetic metal-organic framework (MOF) as a novel sorbent, and its optimization by experimental design methodology for determination of palladium in environmental samples. Talanta 99:132–139

Balkus JK, Ly KT (1991) The preparation of an X type zeolite. J Chem Educ 68(10):875–877

Cheng Q, Yang W, Li Z, Zhu Q, Chu T, He C, Fang C (2015) Adsorption of gaseous radioactive iodine by Ag/13X zeolite at high temperatures. J Radioanal Nucl Chem 303:1883–1889

Collins FM, Lucy AR, Sharp C (1997) Desulphurisation of oils via hydrogen peroxide and heteropolyanion catalysis. J Mol Catal A Chem 117:397–403

Dutta S (2013) Optimization of Reactive Black 5 removal by adsorption process using Box–Behnken design. Desalination Water Treat 51(40–42):7631–7638

Gong YJ, Dou T, Kang SJ, Li Q, Hu YF (2009) Deep desulfurization of gasoline using ion-exchange zeolites: Cu (I)-and Ag (I)-beta. Fuel Process Technol 90:122–129

Gutiérrez OY, Singh S, Schachtl E, Kim J, Kondratieva E, Hein J, Lercherv JA (2014) Effects of the support on the performance and promotion of (Ni)MoS2 catalysts for simultaneous hydrodenitrogenation and hydrodesulfurization. Catalysis 4:1487–1499

Hernandez-Maldonado AJ, Yang RTJ (2004) Desulfurization of diesel fuels by adsorption via π-complexation with vapor-phase exchanged Cu (I)-Y zeolites. Am Chem Soc 126:992–993

Hernández-Maldonado AJ, Yang RT (2003) Desulfurization of liquid fuels by adsorption via π-complexation with cu(i)-y and ag-y zeolites. Ind Eng Chem Res 42:123–129

Houthoofd K, Grobet PJ, Jacobs PA (2008) Study of the adsorption of organic molecules on transition metal exchanged zeolites via solid state NMR. Part 2: adsorption of organic molecules on zeolite NaX, CaX, and CaCoX. J Phys Chem B 112:9630–9640

Irvine RL (1998) Process for desulfurizing gasoline and hydrocarbon feedstocks. U.S. Patent 5,730,860

Kostinko JA (1982) Factors influencing the synthesis of zeolites A, X, and Y. Intrazeolite Chem 1:1–17

Kumar DR, Srivastava VC (2012) Studies on adsorptive desulfurization by activated carbon. Clean Soil Air Water 40:545–550

Kumar A, Prasad B, Mishra IM (2008) Optimization of process parameters for acrylonitrile removal by a low-cost adsorbent using Box–Behnken design. J Hazard Mater 150:174–182

Laborde-Boutet C, Joly G, Magnoux P, Nicolaos A, Thomas M (2006) Selectivity of thiophene/toluene competitive adsorptions onto zeolites. Influence of the alkali metal cation in FAU (Y). Ind Eng Chem Res 45:8111–8116

Ma X, Velu S, Kim JH, Song C (2002) Deep desulfurization of gasoline by selective adsorption over solid adsorbents and impact of analytical methods on ppm-level sulfur quantification for fuel cell applications. Catal Today 77:107–116

Ma X, Sun L, Song C (2005) A new approach to deep desulfurization of gasoline, diesel fuel and jet fuel by selective adsorption for ultra-clean fuels and for fuel cell applications. Appl Catal B 56:137–147

Moattar F, Hayeripour S (2004) Application of Chitin and Zeolite adsorbents for treatment of low level radioactive liquid wastes. IJEST 1:45–50

Mourabet M, El Rhilassi A, El Boujaady H, Bennani-Ziatni M, El Hamri R, Taitai A (2012) Removal of fluoride from aqueous solution by adsorption on Apatitic tricalcium phosphate using Box–Behnken design and desirability function. Appl Surf Sci 258:4402–4410

Ogunlaja A, Coombes M, Torto N, Tshentu Z (2014) The adsorptive extraction of oxidized sulfur-containing compounds from fuels by using molecularly imprinted chitosan materials. React Funct Polym 81:61–76

Qin Y, Mo Zh, Yu W, Dong Sh, Duan L, Gao X, Song L (2014) Adsorption behaviors of thiophene, benzene, and cyclohexene on FAUzeolites: comparison of CeY obtained by liquid-, and solid-state ion exchangeYucai. Appl Surf Sci 292:5–15

Salmasi M, Fatemi S, Rad MD, Jadidi F (2013) Study of carbon dioxide and methane equilibrium adsorption on silicoaluminophosphate-34 zeotype and T-type zeolite as adsorbent. IJEST 10:1067–1074

Shams A, Dehkordi AM, Goodarznia I (2008) Desulfurization of liquid-phase butane by zeolite molecular sieve 13x in a fixed bed: modeling, simulation, and comparison with commercial-scale plant data. Energy Fuels 22:570–575

Shi Y, Zhang W, Zhang H, Tian F, Jia C, Chen Y (2013) Effect of cyclohexene on thiophene adsorption over NaY and LaNaY zeolites. Fuel Process Technol 110:24–32

Song H, Cui XH, Song HL, Jao HJ, Li F (2014) Characteristic and adsorption desulfurization performance of Ag–Ce bimetal ion-exchanged Y zeolite. Ind Eng Chem Res 53:14552–14557

Song H, Jiang B, Song HL, Jin Z, Sun X (2015) Preparation of AgY zeolite and study on its adsorption equilibrium and kinetics. Res Chem Intermed 41(6):3837–3854

Sumathi S, Bhatia S, Lee KT, Mohamed AR (2009) Optimization of microporous palm shell activated carbon production for flue gas desulphurization: experimental and statistical studies. Bioresour Technol 100:1614–1621

Tian F, Shen Q, Fu Z, Wu Y, Jia C (2014) Enhanced adsorption desulfurization performance over hierarchically structured zeolite Y. Fuel Process Technol 128:176–182

Wajima T, Ikegami Y (2009) Synthesis of crystalline zeolite-13X from waste porcelain using alkali fusion. Ceram Int 35:2983–2986

Yang RT (2003) Adsorbents: fundamentals and applications. Wiley, New York

Yang RT, Hernandez-Maldonado AJ (2003) Desulfurization of transportation fuels with zeolites under ambient conditions. Science 301:79–81

Yang RT, Takahashi A, Yang FH, Hernández-Maldonado A (2002) U.S. and foreign patent applications filed

Yi D, Huang H, Meng X, Shi L (2013) Desulfurization of liquid hydrocarbon streams via adsorption reactions by silver-modified bentonite. Ind Eng Chem Res 52:6112–6118

Yong Y, Liu X, Xu B (2014) Recent advances in molecular imprinting technology for the deep desulfurization of fuel oils. New Carbon Mater 29(1):1–14

Zepeda TA, Infantes-Molina A, Díaz de León JN, Fuentes S, Alonso-Núñez G, Torres-Otañez G, Pawelec B (2014) Hydrodesulfurization enhancement of heavy and light S-hydrocarbons on NiMo/HMS catalysts modified with Al and P. Appl Catal A Gen 484:108–121

Zhang X, Tang D, Zhang M, Yang R (2013) Synthesis of NaX zeolite: influence of crystallization time, temperature and batch molar ratio SiO_2/Al_2O_3 on the particulate properties of zeolite crystals. Powder Technol 235:322–328